Naunyn-Schmiedeberg's Archives of Pharmacology
https://doi.org/10.1007/s00210-020-01879-1

ORIGINAL ARTICLE

Physicochemical characterization and cytotoxicity of articaine-2-hydroxypropyl-β-cyclodextrin inclusion complex

Jonny Burga-Sánchez[1] · Luiz Eduardo Nunes Ferreira[2] · Maria Cristina Volpato[1] · Luis Fernando Cabeça[3] · Mario Braga[4] · Leonardo Fernandes Fraceto[5] · Eneida de Paula[4] · Francisco Carlos Groppo[1]

Received: 27 August 2019 / Accepted: 22 April 2020

Abstract

Articaine (ATC) is one of the most widely used local anesthetics in dentistry. Despite its safety, local toxicity has been reported. This study aimed to develop an ATC-2- hydroxypropyl-β-cyclodextrin inclusion complex (ATC HPβCD) and to assess its toxicity in vitro. The inclusion complex was performed by solubilization, followed by a fluorimetric and job plot assay to determine the complex stoichiometry. Scanning electron microscopy, DOSY- 1 H-NMR, differential scanning calorimetry (DSC), and sustained release kinetics were used to confirm the inclusion complex formation. In vitro cytotoxicity was analyzed by MTT assay and immunofluorescence in HGF cells. Fluorimetric and job plot assay determined the inclusion complex stoichiometry (ATC:HPβCD = 1:1) and complex formation time (400 min), as indicated by a strong host/guest interaction (K_a = 117.8 M − 1), complexed fraction (f = 41.4%), and different ATC and ATC HPβCD melting points (172 °C e 235 °C, respectively). The mean of cell viability was 31.87% and 63.17% for 20-mM ATC and 20-mM ATC HPβCD, respectively. Moreover, remarkable cell toxicity was observed with free ATC by immunofluorescence. These results indicate the ATC HPβCD complex could be used to improve the safety of ATC. Further research are needed to establish the anesthetic safety and effectiveness in vivo .

Keywords Hydroxypropyl-β-cyclodextrin · Articaine · Cell viability · Human gingival fibroblast

Introduction

ATC has been pointed out as one of the most potent and less toxic local anesthetic in dentistry (Pellicer-Chover et al. 2013; Kambalimath et al. 2013; Tortamano et al. 2013). However, despite its high anesthetic success rate, there are reports of increased risk of paresthesia, changes in sensitivity, and transient postoperative pain have been related (Malamed et al. 2001; Garisto et al. 2010; Moore and Haas 2010; Pogrel 2012; Kämmerer et al. 2013). In fact, an analysis of reports

✉ Jonny Burga-Sánchez
jonnyburga@gmail.com

Luiz Eduardo Nunes Ferreira
luiz.enferreira@gmail.com

Maria Cristina Volpato
volpato@fop.unicamp.br

Luis Fernando Cabeça
lfcabeca@yahoo.com.br

Mario Braga
marioabraga@hotmail.com

Leonardo Fernandes Fraceto
leonardo@sorocaba.unesp.br

Eneida de Paula
depaula@unicamp.br

Francisco Carlos Groppo
fcgroppo@fop.unicamp.br

[1] Department of Physiological Sciences, Piracicaba Dental School, University of Campinas – UNICAMP, Avenida Limeira, 901, Piracicaba, SP 13414-903, Brazil

[2] Laboratory of Inflammation and Immunology, Guarulhos University, Praça Teresa Cristina, 229 - Centro, Guarulhos, SP 07023-070, Brazil

[3] Parana Federal Technological University – Londrina City, Avenida dos Pioneiros 3131, Jd Morumbi, Londrina, PR 86036-370, Brazil

[4] Department of Biochemistry, Biology Institute, University of Campinas – UNICAMP, Rua Monteiro Lobato, 255, Campinas, SP 13083-862, Brazil

[5] Laboratory of Environmental Nanotechnology, Institute of Science and Technology of Sorocaba, São Paulo State University (UNESP), Av. Três de Março, 511 - Aparecidinha, Sorocaba, SP 18087-180, Brazil

Published online: 05 May 2020

to the FDA Adverse Event Reporting System showed the articaine as one of the two local anesthetics that generates a signal of paresthesia, especially in dentistry (Piccinni et al. 2015). This adverse effect has been attributed to the local toxicity caused by the high concentration of ATC on the anesthetic solution (Haas and Lennon 1995; Haas 2006).

In that way, studies in recent years using cyclodextrins (CDs) as cell carriers and solubilizers of local anesthetics have been carried out to improve the pharmacological features of these drugs (Prado et al. 2017) and to reduce this side effect (Araújo et al. 2005; de Paula et al. 2010a). CDs are cyclic oligosaccharides of glucopyranose units (6, 7, 8 for α, β, and γ, respectively) linked by α (1, 4) linkages. Although the entire CD molecule is water-soluble, these units form a truncated cone with a hydrophobic (nonpolar) internal cavity allowing the binding of the hydrophobic drug radicals compatible with the cavity size (6.0–6.5 Å) and keeping a hydrophilic outer surface (Loftsson and Duchêne 2007). The 2-hydroxypropyl-β-cyclodextrin (HPβCD), a synthetic βCD, has received special attention because of its safety, even in parenteral use, since it does not permeate the cell membrane, making it suitable for several administration routes. It has a much higher aqueous solubility (> 600 mg/mL) that differs from the original βCD (18.5 mg/mL). HPβCD has been approved in several markets and do not cause immune response in mammals. Moreover, because of its cavity size, it is appropriate for drug molecules with aromatic rings (Davis and Brewster 2004; Loftsson and Duchêne 2007).

Thus, the objective of this study was to perform the characterization of the ATC as a guest molecule into the host cavity of HPβCD and evaluate the cytotoxicity in vitro of this novel inclusion complex.

Methods

Preparation of the solid $ATC_{HP\beta CD}$

The inclusion complex was prepared as described before (Moraes et al. 2007a; Araújo et al. 2008). Briefly, equimolar amounts of ATC HCl (MW = 320.84 g/mol) (DFL Industria e Comércio S.A., Rio de Janeiro, Brazil) and HPβCD (MW = 1400 g/mol) (Kleptose HP®, Roquette Serv. Tech. Lab. Lestrem, Cedex, France), in a 1:1 M ratio, were dissolved in ultrapure water (Milli-Q® Direct 8, Merck-Millipore, Germany) at room temperature (25 ± 1 °C) for 24 h by continuous stirring to achieve complete solubilization. The solution was freeze-dried (Lyo Chamber Guard Christ LCG, Alfa 2–4 LD Plus, Germany) for 72 h and stored at − 20 °C until further use. Physical mixtures were obtained by mixing ATC and HPβCD powders, at the same molar ratio.

Fluorimetric absorption and stoichiometry determination

The interaction between ATC and HPβCD was followed at 272 nm (maximum ATC excitation UV wavelength) using a fluorimeter (Fluorimeter Hitachi F-4500, Japan). The complexation stoichiometry was determined from equimolar solutions of the samples, with ATC spectra recorded in the presence/absence of increasing HPβCD concentrations (ATC:HPβCD molar ratios of 1:0, 1:1, 1:10, 1:20, 1:30, 1:40, 1:50, 1:75, and 1:100) (Sosnowska 1997). Using the job plot analysis (Shafi and Shihry 2009; Braga et al. 2016), ATC spectra were recorded for different ATC:HPβCD molar ratios, remaining the total concentration (M) constant ($M = [ATC]_{total} + [HP\beta CD]_{total} = 2\ \mu M$). As the experiment in the fluorimeter requires UV absorbance solutions between 0.1 and 0.2, low concentrations of the samples were used. All experiments were performed in 5-mM HEPES buffer, at pH 7.4 and 25 ± 2 °C.

The physicochemical parameter analyzed was the maximum fluorescence emission (λ) in the absence (λ_0) and presence (λ) of HPβCD. Data analysis was performed by constructing a plot of $\Delta\lambda$ vs. r, according to the following formulas:

$$\Delta\lambda = \lambda - \lambda_0 \quad (1)$$

$$r = \frac{[ATC]}{\{[ATC]_{total} + [HP\beta CD]_{total}\}} \quad (2)$$

For a given value of r, the concentration of the complex ATC:HPβCD will reach a maximum corresponding to the point which the derivative d[ATC: HPβCD]/dr = 0. The maximum value for this parameter occurs at $r = 0.5$ which indicates a 1:1 stoichiometry. Changes in the fluorimetric shift will be proportional to the complex concentration and it is possible to plot these changes against r (Loukas et al. 1998).

NMR analyses

ATC, HPβCD, and $ATC_{HP\beta CD}$ samples were diluted in D_2O, and 600 μL aliquots were transferred to 5-mm tubes for spectrum acquisition. One and two dimensional ^{1}H-NMR spectra were determined at 25 °C on Varian INOVA 500 spectrometer (11.75 T frequency) and 499.73 MHz (digital resolution of measurements of 0.39 Hz/point), at the Brazilian Synchrotron Light Laboratory (LNBio, Campinas, Brazil). The residual water peak (4.8 ppm) was used as an internal reference. In all experiments, the suppression of residual water was made by the pre-saturation technique. Data were processed using the nmrPIPE/nmrVIEW program (ACD/Labs, Toronto, Canada).

The diffusion experiments (DOSY) were conducted to ATC (5 mM), HPβCD (5 mM), and 1:1 ($ATC_{HP\beta CD}$) at

25 °C. The sequence used was the Dbppste. The total duration of the gradient pulse was 2 ms, the standby time of diffusion was 0.05 s, and the minimum gradient force was 0.3 G/cm (Loukas et al. 1998; Laverde t al. 2002; Braga et al. 2016). For all experiments, 30 spectra (64 transients each) were collected with gradient pulses with amplitudes ranging from 0.68×10^{-3} to 3.4×10^{-3}T/cm, in which were observed an approximately 100% decay in intensity of the resonance. This phenomenom was found in the biggest gradient amplitude.

The fraction of complexed drug (f) was determined as described by the following equation (Braga et al. 2016):

$$f = \frac{D_{\mathrm{ATC}} - D_{\mathrm{Complex}}}{D_{\mathrm{ATC}} - D_{\mathrm{HP\beta CD}}} \quad (3)$$

D_{ATC} = diffusion coefficient of free ATC; D_{Complex} = $\mathrm{ATC_{HP\beta CD}}$ inclusion complex diffusion coefficient; and $D_{\mathrm{HP\beta CD}}$ = diffusion coefficient of free HPβCD.

The affinity constant was calculated from the last equation deduced from the equilibrium constant for the 1:1 stoichiometry ATC: HPβCD as follows (Arantes et al. 2009):

$$K_{\mathrm{a}} = \frac{f}{(1-f)\left([HP\beta CD] - f[ATC]\right.} \quad (4)$$

The f is the ATC complexed fraction, [ATC] = initial ATC concentration (M); [HPβCD] = initial HPβCD concentration (M).

Differential scanning calorimetry (DSC)

DSC curves were obtained with a DSC-Q100 (TA Instruments Waters, USA), using 50 mL/min nitrogen rate flow and 15 °C/min heating rate over a range of 0–300 °C. Five-milligram samples (ATC, HPβCD and 1:1 $\mathrm{ATC_{HP\beta CD}}$) were placed in aluminum pans. The temperature was calibrated with indium element, and an empty pan was used as reference.

Sustained release kinetics and accelerated stability assessment

In vitro release experiments were carried out using a two-compartment system, with a cellulose membrane (Spectrapore, MWCO 1000 Da) to separate the donor (1-mL ATC or $\mathrm{ATC_{HP\beta CD}}$ sample) and the acceptor (100 mL of ultrapure water) compartments, under continuous stirring. Aliquots were withdrawn from the acceptor compartment at regular intervals, and ATC concentration was determined by HPLC according to a previously validated method (Franz-Montan et al. 2015). Furthermore, three samples (10 mg each) of $\mathrm{ATC_{HP\beta CD}}$ were submitted for 6 months to challenge conditions (40 °C ± 2 °C and HR = 75% ± 5%) in a climatic chamber (Tecnal, TE-4003 – Brazil) to achieve the compound stability. The release data were evaluated using the zero order, first order, Higuchi, and Korsmeyer-Peppas models (Ramteke et al. 2014).

Scanning electron microscopy (SEM)

Lyophilized samples of $\mathrm{ATC_{HP\beta CD}}$, ATC, HPβCD, and their physical mixture were fixed on aluminum stubs with double-sided carbon tape. The samples were metallized with gold under vacuum for 120 s. Images were analyzed using a scanning microscope (JSM 5800LV, JEOL, Japan) in order to observe possible structural changes on the ATC and HPβCD crystals after complexation.

Cytotoxicity by MTT reduction and immunofluorescent assay

Cell culture process

Spontaneously immortalized human gingival fibroblast (HGF) cells were maintained in a monolayer culture in 95% air and 5% CO_2 at 37 °C in DMEM supplemented with 10% fetal bovine serum, 1% penicillin/streptomycin, and 3-μg/mL amphotericin B (Fungizone® GIBCO, USA).

Cell proliferation and function assay (Vybrant® MTT proliferation assay)

The MTT Cell Proliferation Assay kit (Molecular Probes Life Technologies, USA) was used and adapted to a previously described method (Mosmann 1983). Briefly, 2×10^4 cells/well were seeded in a 96-well plate with 200 μL of DMEM culture medium (Vitrocell Embriolife, Brazil) supplemented with 10% FBS. After 48 h, HGF cells were exposed to different ATC and $\mathrm{ATC_{HP\beta CD}}$ concentrations for 45 min. Then, the supernatant was removed and 200-μL DMEM medium containing MTT 0.3 mg/mL was added in each well. Cells were incubated for 3 h in 95% air and 5% CO_2 at 37 °C, protected from light. The supernatant was removed and cells were gently washed twice with PBS pH 7.4, and 200 μL of absolute ethanol were added to each well. Finally, absorbance was measured at 570 nm in a microspectrophotometer (ASYS UVM340; Biochrome, England).

Immunofluorescence cell morphology assay

The double immunofluorescence staining assay was performed according to the manufacturer. Briefly, 5×10^2 HGF cells were grown on previously poly-L-lysine-treated coverslips, fixed with 4% formaldehyde and permeabilized with 0.2% Triton X-100. F-actin filaments were labeled with Alexa Fluor® 488 phalloidin (ThermoFisher Scientific, Oregon, USA), and nuclei were stained with Hoechst 33342

(ThermoFisher Scientific). Then, coverslips were mounted on slides using Entellan® new reagent (Sigma-Aldrich, USA). The multiple-exposure image was acquired on a Leica DMR microscope equipped with an epifluorescence camera DFC345FX (Leica, Germany) at × 20 with a fluorescence excitation (Ex) and emission (Em) maxima of 495 nm/518 nm. DMEM was used as cell positive control with no effect on cellular morphology and Triton X-100 as a negative control since it causes lysis on cell membrane.

Statistical analyses

Data were tested for normal distribution by Shapiro-Wilks test and Levene was used to test the equivalency of variances. Analyses of variance (ANOVA) followed by Tukey test (post hoc analysis) were applied for cell viability assay (MTT). Significance level was set at 1% ($\alpha = 0.01$). All analyzes were performed using the Biostat® 5.0 (Mamirauá Institute, PA, Brazil) and GraphPad Prism 6.0 (GraphPad Software, Inc., La Jolla, CA, USA) software.

Results

ATC fluorimetric absorption properties and complexation

The variation of fluorescence intensity was proportional to the concentration of the complex and could be plotted against *r*. Even though the molar quantity of HPβCD increased from one to 100, all of the curves showed a similar distribution as 1:1 (Fig. 1). As the total molar concentrations of ATC and HPβCD were equal (1 μM), the *r*-value obtained was 0.5, as seen on Fig. 2a, which indicates a complexation molar ratio ATC:HPβCD = 1:1. When plotted the area under the curve (AUC) of the 1:1 complex over 24 h revealed an equilibration time of 400 min at the plateau. The kinetics of complex formation is directly related to the hydrophobicity of the guest molecule to be incorporated, and there was no increase in the absorbance after 400 min (Fig. 2b).

NMR experiments

Table 1 summarizes the ATC shift variation. The great variation can be observed for H_7, H_8, and H_9. The confirmation of the complex was done through experiments of DOSY. Figure 3 shows the ^{1}H-NMR spectra of the ATC and HPβCD molecule, observing a right displacement of the curve.

Diffusion measures

Once the supramolecular complexation characterization was performed (analysis via complexation stoichiometry and probable $ATC_{HP\beta CD}$ structure), diffusion experiments were performed in order to measure the ATC complexed fraction via NMR, as well as association constant (K_a) between ATC and HPβCD. These values, carried out from Eqs. 1–4, are shown on Table 2.

As shown on Table 2, the diffusion of the anesthetic molecule in solution (D_{ATC}) is greater than the HPβCD ($D_{HP\beta CD}$) due to the difference in molecular weight of both compounds, indicating that the mobility of these molecules in solution are different. From Eq. 3 and 4, the values of the complexed fraction ($f = 41.41\%$) and the affinity constant ($K_a = 117.8\ M^{-1}$) were obtained, respectively.

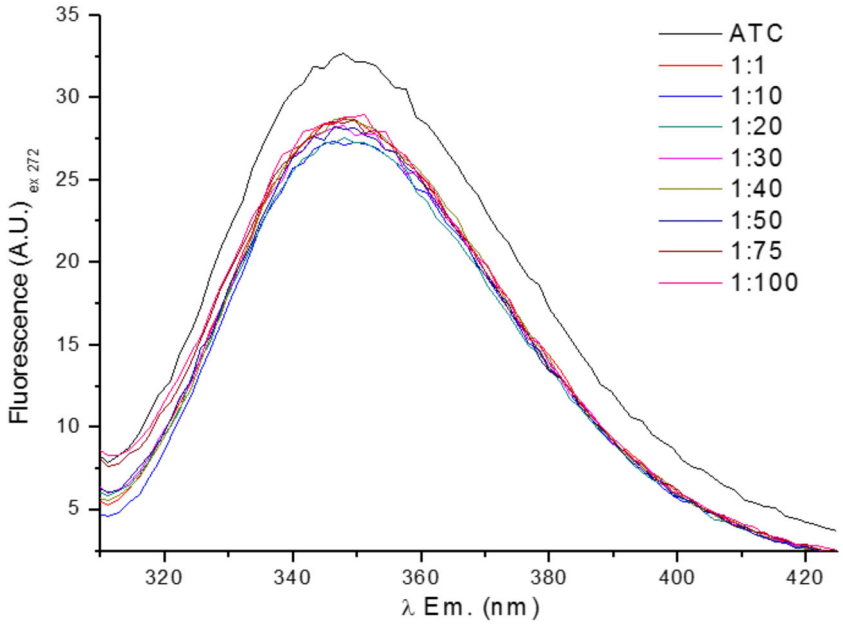

Fig. 1 Fluorescence emission spectra of the $ATC_{HP\beta CD}$ at 1:1 to 1:100 (ATC:HPβCD) concentration

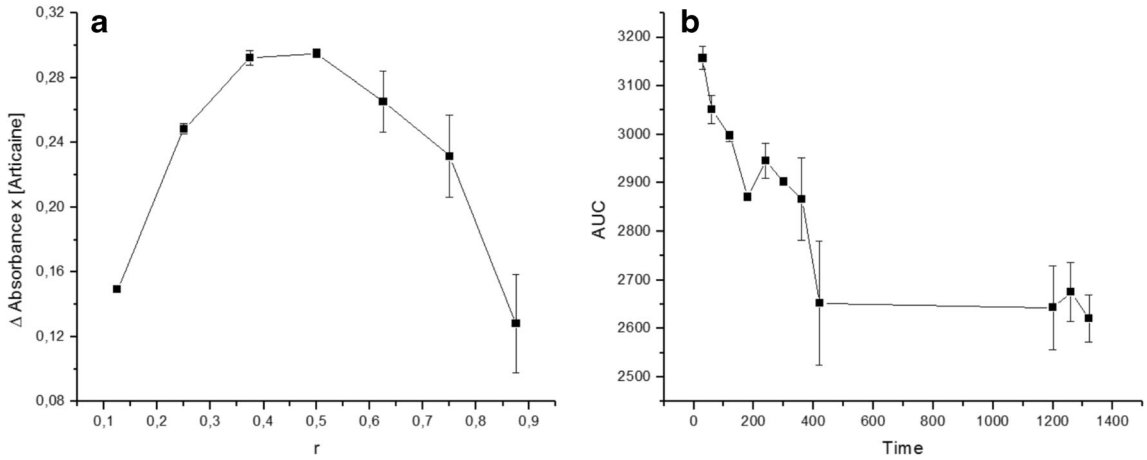

Fig. 2 **a** Job plot changes in fluorescence intensity at different ATC:HPβCD molar ratios (*r*) for determination of the stoichiometry of complexation as described in methods; 5-mM HEPES buffer, at pH 7.4 and 25 ± 2 °C (*n* = 3, mean ± SD). **b** Kinetics of complexation of ATC and HPβCD (*n* = 3, mean ± SD); each point represents the area under the curve generated by fluorimetry in the formation of the equimolar complex (1:1) in different time points during 24 h

Differential scanning Calorimetry

Thermograms of plain ATC and $ATC_{HP\beta CD}$ inclusion complex are shown in Fig. 4. The lack of ATC peak on melting point (172–173 °C) on the curve when complexed with HPβCD is a strong evidence of the new inclusion compound formation (Yilmaz et al. 1995; Novak et al. 1998; Meier et al. 2001).

Sustained release kinetics and accelerated stability

The inclusion of ATC in the HPβCD cavity reduced the in vitro release of ATC, as shown in Fig. 5. After 240 min, the maximum release percentage was 84.5 ± 3.3% (ATC at 0 months), 72.5 ± 1.1% ($ATC_{HP\beta CD}$ at 0 months), and 76.9 ± 1.7% ($ATC_{HP\beta CD}$ at 6 months). At the end releasing point, there was a significant difference between ATC and the complex formulations ($p < 0.05$, ANOVA-Tukey). No difference was observed between $ATC_{HP\beta CD}$ 0 months and $ATC_{HP\beta CD}$ 6 months. The in vitro drug release profile was applied in different mathematical models used for drug delivery. The Higuchi model exhibited the highest correlation coefficient (r^2) for the different formulations (Table 3). This suitable model revealed the release of ATC from the formulations, which implies the release of drug from the complex as a process that depends of the square root of time and that diffusion may be controlled (Fig. 5). The constant rate was 8.4240 and 7.6142 for ATC and $ATC_{HP\beta CD}$ 0 months, respectively. These values were significantly different ($p < 0.05$, ANOVA-Tukey).

Table 1 Chemical shift of ATC ^{1}H and ATC in the inclusion complex $ATC_{HP\beta CD}$

H	ATC (ppm)	$ATC_{HP\beta CD}$ (ppm)	Δδ (ppm)
2	1.008	0.902	0.106
3	1.713	1.605	0.108
5	2.116	2.020	0.096
6	3.033	2.919	0.114
7	3.100	2.985	0.115
8	3.871	3.771	0.100
9	4.255	4.139	0.116
10	7.516	7.418	0.098

Scanning electron microscopy (SEM)

The crystals of HPβCD have hemispherical forms of tens of microns, smooth surface, and aligned contours. The ATC crystals are grouped with prismatic shapes and straight edges. The $ATC_{HP\beta CD}$ has a completely different structure from amorphous laminar appearance of hundreds of microns (Fig. 6).

Cytotoxicity and immunofluorescent assay

The HGF cells' metabolic activity was affected significantly when treated with concentrations above 5 mM of plain ATC and $ATC_{HP\beta CD}$ for 45 min, with a lower cytotoxicity tendency in the complexed group. Although lower concentrations of both ATC and $ATC_{HP\beta CD}$ showed similar cytotoxic profile, 20-mM plain ATC was significantly ($p < 0.01$) more cytotoxic in comparison with 20-mM $ATC_{HP\beta CD}$. The mean (± SD) of cell viability for 20-mM ATC and 20-mM $ATC_{HP\beta CD}$ was 31.87% (± 9.69) and 63.17% (± 13.34), respectively (Fig. 7). The HPβCD did not affect the cell viability.

A loss of cytoplasm volume and apoptotic body formation were found in HGF cells treated with 5-mM plain ATC, indicating the cytotoxic effect of this local anesthetic. These

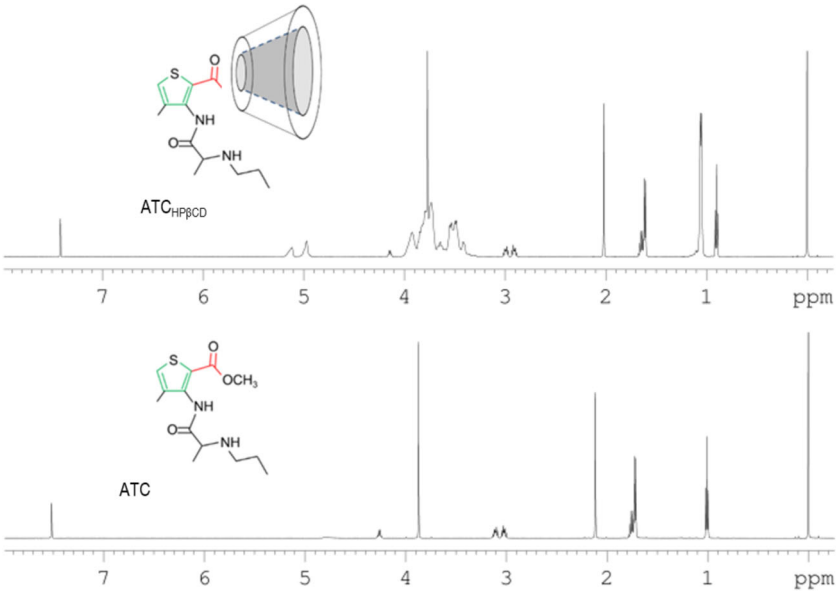

Fig. 3 ^{1}H-NMR spectrum (400 MHz, D_2O/reference residual H_2O at 4.81 ppm) to $ATC_{HP\beta CD}$ complex (**a**) and ATC sample (**b**)

effects were observed with lower intensity on the groups treated with $ATC_{HP\beta CD}$ at the same ATC concentration (Fig. 8).

Discussion

Great advances in new inclusion complexes using HPβCD as a delivery drug system of local anesthetics have been reported (Fréville et al. 1996; Kopecký et al. 2004; Moraes et al. 2007a, b; Franco de Lima et al. 2012; Cereda et al. 2012; Vermet et al. 2014; Serpe et al. 2014; Prado et al. 2017). To identify this complexation, changes in the UV absorption spectra have been suggested (Misiuk and Zalewska 2011). The fluorescence reduction of ATC in the presence of HPβCD (Fig. 1) was very similar in all the molar ratios assessed, reflecting the alteration of the polarity of the environment or by the collision of the fluorophore with inclusion complex. This altered fluorescence was also observed with tetracaine, oxethazaine, and other guest molecules. According to the job plot analysis (Fig. 2), in which the maximum occurred at $r = 0.5$ (Eq. 2), the complexation stoichiometry was confirmed to be 1:1. Similar results have been obtained with ropivacaine, tetracaine, and oxethazaine (Moraes et al. 2007a; Braga et al. 2016; Prado et al. 2017).

Table 2 Diffusion coefficient (D) of ATC, HPβCD, and $ATC_{H\beta CD}$

Samples	D ($10^{-10}m^2s^{-1}$)	Complex molar fraction (f)%	K_a mol/l
ATC	4.69 ± 0.040	–	–
HβCD	2.42 ± 0.011	–	–
$ATC_{H\beta CD}$	3.75 ± 0.022	41.41	117.8

Associated constant (Ka) and complexed fraction (f) of ATC on the $ATC_{H\beta CD}$ complex

The NMR spectroscopy is one of the most informative techniques for the study of CD complexes with several compounds providing direct evidence of the formation complexes. The presence of the guest molecule, when inserted into the inner cavity of the CDs, produces changes in the chemical environment of the internal hydrogens (H_3 and H_5), but not in the external hydrogens (H_1, H_2 and H_4) (Pinto et al. 2005). In addition, the interaction of the host molecule with the CD cavity can cause variation in chemical shift of hydrogens of incorporated molecule in the cavity (Xiliang et al. 2003; Bratu et al. 2005). Thus, NMR data led to the determination of the ATC:HPβCD association constant ($K_a = 117.8$ M^{-1}), which indicates a stable affinity between these compounds. This outcome is even higher than other amide local anesthetics when complexed to HPβCD such as S-bupivacaine ($K_a = 91$ M^{-1}), S-ropivacaine ($K_a = 55$ M^{-1}), and prilocaine ($K_a = 41$ M^{-1}) determined by this method (de Paula et al. 2010b; Cabeça et al. 2011). Similarly, it has been shown a $K_a = 198$ M^{-1}

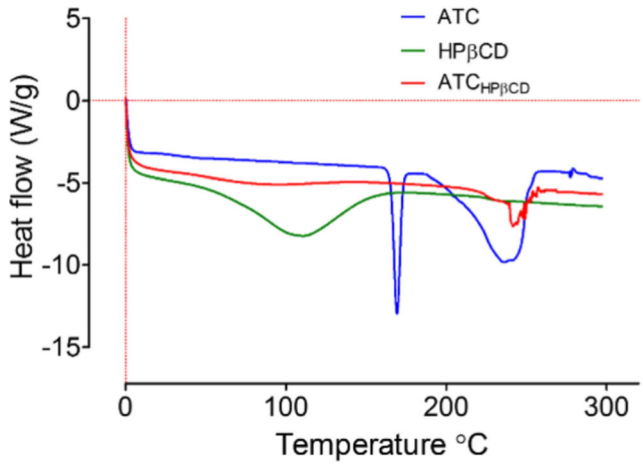

Fig. 4 Thermograms of ATC, HPβCD, and $ATC_{HP\beta CD}$ (1:1 M ratio)

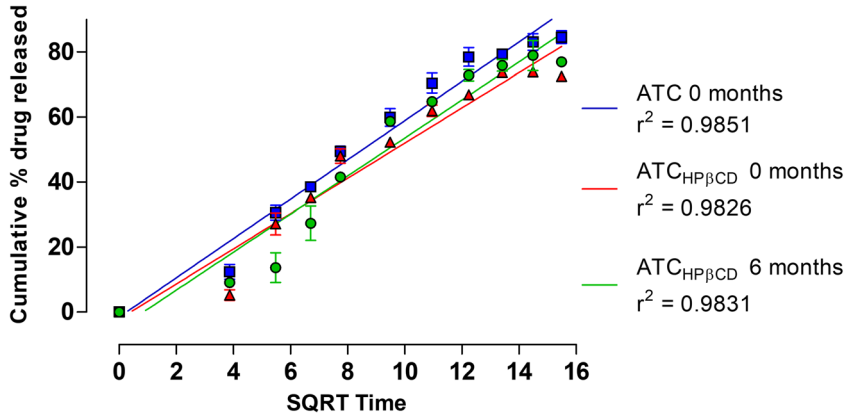

Fig. 5 Higuchi model kinetics for articaine formulations release (cumulative percent drug released vs. square root of time). SQRT indicates square root. ATC and $ATC_{HP\beta CD}$ measured at 25 °C and pH 7.4 ($n = 3$, mean ± SD)

between the oxethazaine and HPβCD (Prado et al. 2017). Since K_a is directly related to the drug lipophilicity, high association between these compounds was expected.

DSC is a common thermal technique used in research of solid-state interactions between drugs and CDs (Giordano et al. 2001; Mura et al. 2003). The comparison of the thermal curves of single compounds, their physical mixture, and the apparent inclusion complex provides insight about the interactions between the components as consequence of the process used for the complex preparation (Mura 2015). As seen with the inclusion complex between ropivacaine-HPβCD and lidocaine-HPβCD, there was the disappearance of the ATC melting peak when complexed with HPβCD in the DSC curve (Araújo et al. 2008). The increased temperature of decomposition observed in the complex is a clear signal of the increased drug thermal stability because of the ATC inclusion inside the HPβCD cavity (Yilmaz et al. 1995; Novak et al. 1998; Meier et al. 2001).

The most widely used in vitro method to evaluate the release of a drug is through a vertical diffusion cell, using a cellulose permeable membrane by which the release of a drug is assessed over time (Shen and Burgess 2012). As recommended before for local anesthetics (Prado et al. 2017), free ATC showed a release above 80%. However, samples of $ATC_{HP\beta CD}$ did not achieve that percentage release after 4 h, and this phenomenon could be explained by the high complexed fraction of ATC on HPβCD (41.41%) and the strong and stable affinity of this inclusion complex ($K_a = 117.8\ M^{-1}$). Moreover, it is possible to observe that there was a decrease in the values of release constants for the different formulations since the 6 months' formulation showed a higher release constant than the newly prepared complex, but still with a lower value than the non-complex formulation (Table 3). Also, the in vitro drug release profile was applied in different mathematical models and evaluated by correlation coefficient (r^2) presented in Table 3. Since the highest degree of correlation coefficient determines the suitable mathematical model that follows drug release kinetics, the Higuchi model fits this point than other models. This finding supports our results since this well-known model has become a prominent kinetic equation in its own for controlled-release formulations and as an important element in drug delivery systems development (Gouda et al. 2017), which implies that release of drug from the complex as a square root of a time-dependent and diffusion-controlled process (Fig. 5). Interestingly, the $ATC_{HP\beta CD}$ inclusion complex submitted to challenge conditions for 6 months showed a similar releasing curve as the original complex (0 months) indicating a good compound stability. All these results suggest the complex as a controlled drug releaser, modifying the drug permeation across cell membrane and increasing the bioavailability of the original molecule.

Table 3 Correlation coefficients (r^2) and constant values for the different mathematical models applied to the release of ATC

	Mathematical models								
	Zero order		First order		Higuchi		Korsmeyer-Peppas		
Formulations	k (h^{-1})	r^2	k ($10^{-3}\ h^{-1}$)	r^2	k ($h^{-1/2}$)	r^2	k (h^{-1})	n	r^2
ATC 0 months	0.6108	0.9404	8.225	0.7949	8.4240	0.9851	1.1430	0.3363	0.9582
$ATC_{HP\beta CD}$ 0 months	0.4846	0.8659	6.891	0.6142	7.6142*	0.9826	0.8011	0.3187	0.8573
$ATC_{HP\beta CD}$ 6 months	0.5732	0.9533	7.112	0.9333	8.0122	0.9831	0.9082	0.3295	0.9648

*Statistical difference in relation to ATC 0 months, $p < 0.05$, ANOVA-Tukey

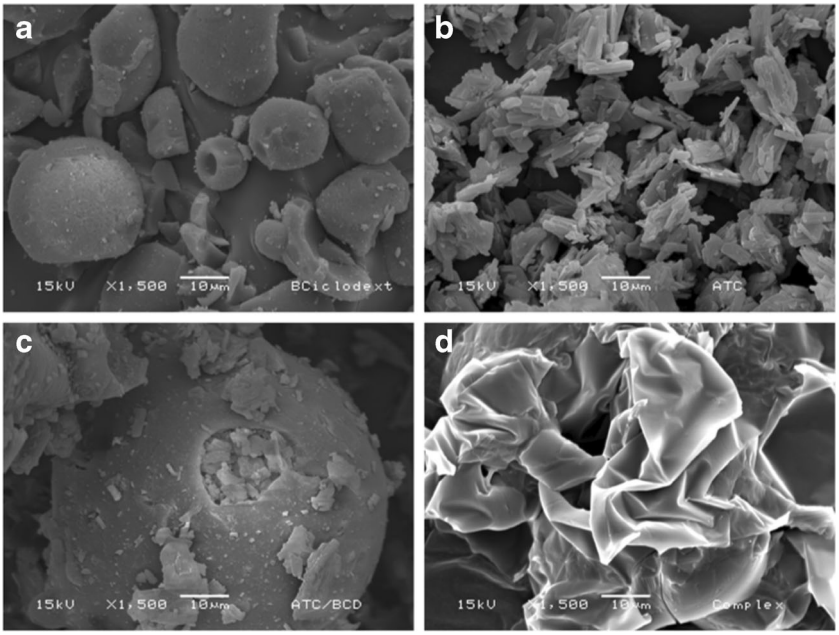

Fig. 6 Scanning electron microscopy of **a** natural HPβCD, **b** natural ATC, **c** physical mixture of ATC and HPβCD molar ratio of 1:1, and **d** $ATC_{HP\beta CD}$ inclusion complex molar ratio 1:1. Magnification × 1500, bar = 10 µm

SEM data (Fig. 6) provided evidences of ATC insertion within the cyclodextrin's hydrophobic cavity, since both demonstrate the loss of ATC crystalline pattern in the complex but not in the simple physical mixture of ATC and HPβCD. Similar results were reported for the ropivacaine, tetracaine, and oxethazaine in inclusion complex with HPβCD (Moraes et al. 2007a; Braga et al. 2016; Prado et al. 2017).

On the other hand, the use of HGF cells to assess the cytotoxicity of local anesthetics have been reported, which reveal the HGF as a suitable model for this purpose (Ferreira et al. 2016; Ferreira et al. 2017). The reduction of systemic and/or local toxicity of other local anesthetics has been reported through the inclusion complex with HPβCD. For instance, the complexation of oxethazaine with HPβCD reduced the cytotoxicity and improved the analgesic effect in inflamed tissues, being these notable results considering the instability of local anesthetics on acid environment (Prado et al. 2017). Schawn cells were exposed to complexed and plain bupivacaine and ropivacaine for 24 h (Cereda et al. 2012). Although there were no significant differences on the cytotoxicity effect between these formulations, the authors did not consider the releasing time of the complex and the half-life time of the drugs for this assay. In our study, we considered a 45-min time exposure, since it is the commercial ATC half-life when administered with epinephrine 1:100000 or 1:200000 (Giannakopoulos et al. 2006). The $ATC_{HP\beta CD}$ showed a less cytotoxic trend especially with high concentrations (> 5 mM) of ATC (Fig. 8), maybe because of the observed delayed release and due to the high rate of complexation that prevents direct contact of the active substance (ATC) with the cells. In fact, drug delivery

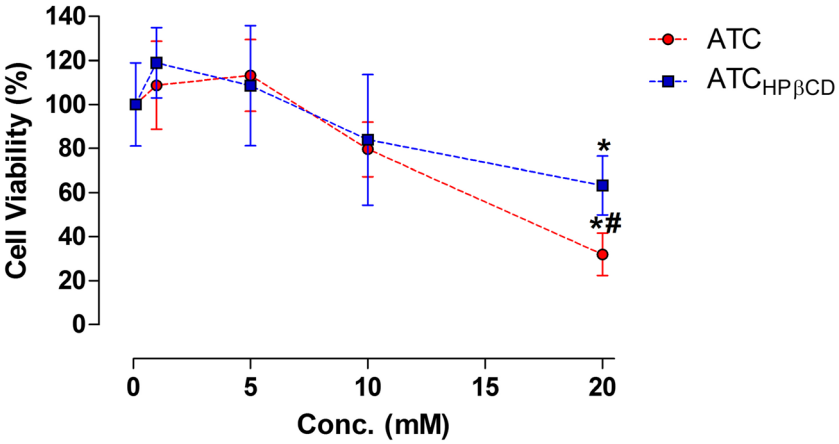

Fig. 7 Viability of HGF cells after treatment with articaine (ATC) and ATC-2-hydroxypropyl-β-cyclodextrin inclusion complex ($ATC_{HP\beta CD}$) for 45 min ($n = 10$, mean ± SD). *Statistical difference between ATC treatments and control (0 mM); #marks significant difference between 20mM ATC and 20-mM $ATC_{HP\beta CD}$, $p < 0.01$ ANOVA, and Tukey test (post hoc)

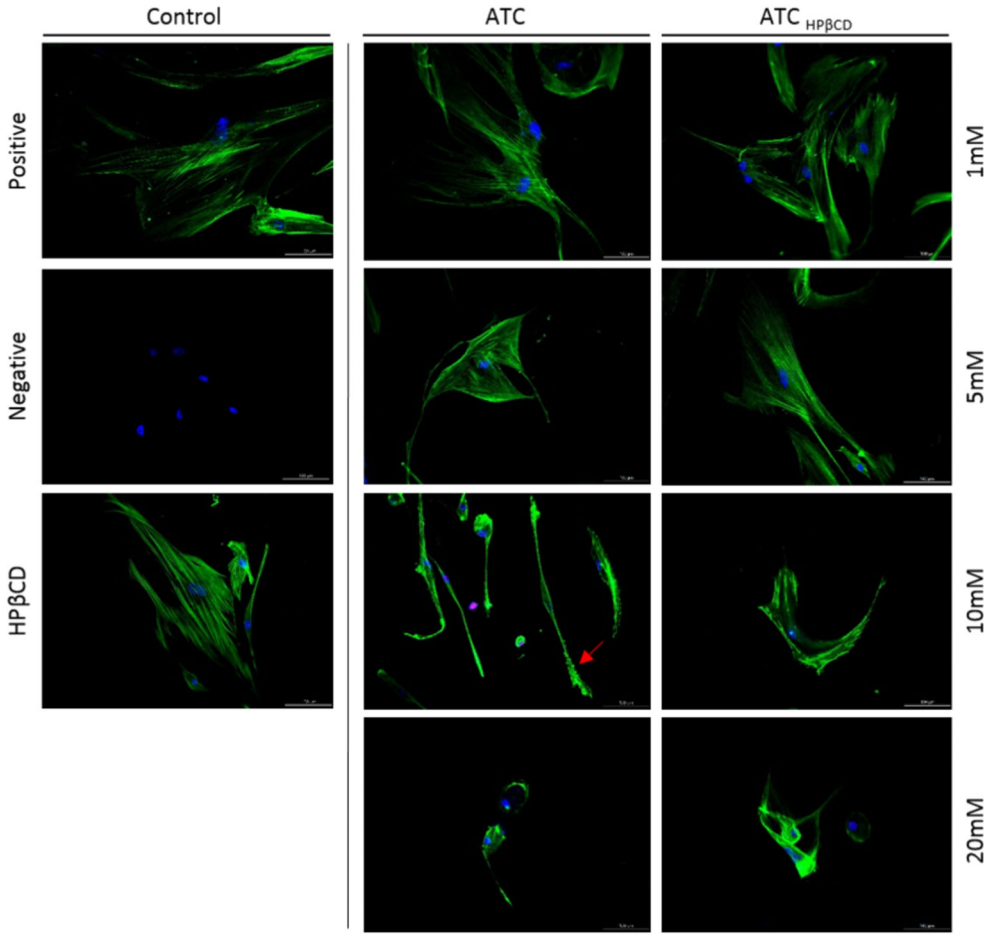

Fig. 8 Effect of plain ATC and the $ATC_{HP\beta CD}$ inclusion complex on HGF cells. A loss of cytoplasm volume and apoptotic bodies (red arrow) can be seen on group treated with 10-mM and 20-mM plain ATC. For positive and negative control groups, DMEM and Triton X-100 0.1% was used, respectively. Magnification × 20, scale bar = 100 μm

systems for local anesthetics act as reservoirs causing slow release of drug, reduce plasma concentration, prolonged the duration of nerve block, and prevent cell toxicity (de Paula et al. 2010a). However, the benefit of the $ATC_{HP\beta CD}$ inclusion complex on cell viability should be further investigated in other cell types.

In conclusion, physicochemical characterization of the $ATC_{HP\beta CD}$ inclusion complex showed a 1:1 (ATC: HPβCD) steady stoichiometry complexation. Diffusion experiments demonstrated a strong and stable affinity between these molecules. The $ATC_{HP\beta CD}$ inclusion complex showed a limited cytotoxic effect in vitro. These results are important for a better understanding of the pharmacological properties of $ATC_{HP\beta CD}$ inclusion complex as a potential and novel alternative for local anesthesia in dental and medical practice, due to the lower cytotoxicity profile. Further research is needed in order to determine the anesthetic safety and effectiveness of this novel inclusion complex.

Acknowledgements We thank PhD. Estefânia Campos and PhD. Jhones Luis Oliveira for the orientation during the DSC and the sustained release kinetics experiments. Also, we thank PhD. Débora Campanella Bastos for the support on immunofluorescence assay.

Author contributions JBS, LENF, and MB contributed with the design the study, literature research, data collection, figure art, and manuscript preparation. LFC, LFF, and EP contributed with drug delivery systems preparation, conducted experiments and manuscript review. FCG and MCV contributed with the design the study, funding acquisition and manuscript review.

Funding information This work was supported by CAPES (Coordenação de Aperfeiçoamento de Pessoal de Nível Superior) and FAPESP (Fundação de Amparo à Pesquisa do Estado de São Paulo), FAPESP #2015/20942-6.

Compliance with ethical standards

Conflict of interest The authors declare that they have no conflict of interest.

References

Arantes LM, Scarelli C, Marsaioli AJ, de Paula E, Fernandes SA (2009) Proparacaine complexation with β-cyclodextrin and p-sulfonic acidcalix[6]arene, as evaluated by varied 1H-NMR approaches. Mag Res Chem 47:757–763. https://doi.org/10.1002/mrc.2460

Araújo DR, Fraceto LF, Braga AFA, de Paula E (2005) Drug-delivery systems for racemic BPV (S50-R50) and BPV enantiomeric mixture (S75-R25): cyclodextrins complexation effects on sciatic nerve blockade in mice. Rev Bras Anestesiol 55:316–328

Araújo DR, Tsuneda SS, Cereda CM, Carvalho FGF, Preté PSC, Fernandes SA, Yokaichiya F, Franco MK, Mazzaro I, Fraceto LF, de F A Braga A, de Paula E (2008) Development and pharmacological evaluation of ropivacaine-2-hydroxypropyl-beta-cyclodextrin inclusion complex. Eur J Pharm Sci 33:60–71. https://doi.org/10.1016/j.ejps.2007.09.010

Braga MA, Martini MF, Pickholz M, Yokaichiya F, Franco MKD, Cabeça LF, Guilherme VA, Silva CM, Limia CE, de Paula E (2016) Clonidine complexation with hydroxypropyl-beta-cyclodextrin: from physico-chemical characterization to in vivo adjuvant effect in local anesthesia. J Pharm Biomed Anal 119:27–36. https://doi.org/10.1016/j.jpba.2015.11.015

Bratu I, Gavira-Vallejo JM, Hernanz A (2005) ^{1}H-NMR study of the inclusion processes for alpha- and gamma-cyclodextrin with fenbufen. Biopolymers 77:361–367. https://doi.org/10.1002/bip.20245

Cabeça LF, Figueiredo IM, de Paula E, Marsaioli AJ (2011) Prilocaine–cyclodextrin–liposome: effect of pH variations on the encapsulation and topology of a ternary complex using ^{1}H-NMR. Magn Reson Chem 49:295–300. https://doi.org/10.1002/mrc.2740

Cereda CM, Tofoli GR, Maturana LG, Pierucci A, Nunes LA, Franz-Montan M, de Oliveira AL, Arana S, de Araujo DR, de Paula E (2012) Local neurotoxicity and myotoxicity evaluation of cyclodextrin complexes of bupivacaine and ropivacaine. Anesth Analg 115:1234–1241. https://doi.org/10.1213/ANE.0b013e318266f3d9

Cs N, Fodor M, Pokol G, Izvekov V, Sztatisz J, Arias MJ, Ginés JM (1998) Investigation of cyclodextrin complexes of mandelic acid. J Therm Anal Calorim 51:1039–1048

Davis ME, Brewster ME (2004) Cyclodextrin-based pharmaceutics: past, present and future. Nat Rev Drug Discov 3:1023–1035. https://doi.org/10.1038/nrd1576

de Paula E, Cereda CM, Tofoli GR, Franz-Montan M, Fraceto LF, Araújo DR (2010a) Drug delivery systems for local anesthetics. Recent Pat Drug Deliv Formul 4:23–34

de Paula E, Araujo DR, Fraceto LF (2010b) Nuclear magnetic resonance spectroscopy tools for physicochemical characterization of cyclodextrin inclusion. In: Hu J (ed) Cyclodextrins chemistry physics. Transworld Research Network, Kerala, pp 1–21

Ferreira LE, Muniz BV, Dos Santos CP, Volpato MC, de Paula E, Groppo FC (2016) Comparison of liposomal and 2-hydroxypropyl-β-cyclodextrin-lidocaine on cell viability and inflammatory response in human keratinocytes and gingival fibroblasts. J Pharm Pharmacol 68:791–802. https://doi.org/10.1111/jphp.12552

Ferreira LE, Muniz BV, Burga-Sánchez J, Volpato MC, de Paula E, Rosa EA, Groppo FC (2017) The effect of two drug delivery systems in ropivacaine cytotoxicity and cytokine release by human keratinocytes and fibroblasts. J Pharm Pharmacol 69:161–171. https://doi.org/10.1111/jphp.12680

Franco de Lima RA, de Jesus MB, Cereda CM, Tofoli GR, Cabeça LF, Mazzaro I, Fraceto LF, de Paula E (2012) Improvement of tetracaine antinociceptive effect by inclusion in cyclodextrins. J Drug Target 20:85–96. https://doi.org/10.3109/1061186X.2011.622400

Franz-Montan M, Baroni D, Brunetto G, Sobral VR, da Silva CM, Venâncio P, Zago PW, Cereda CM, Volpato MC, de Araújo DR, de Paula E, Groppo FC (2015) Liposomal lidocaine gel for topical use at the oral mucosa: characterization, in vitro assays and in vivo anesthetic efficacy in humans. J Liposome Res 25(1):11–19. https://doi.org/10.3109/08982104.2014.911315

Fréville JC, Dollo G, Le Corre P, Chevanne F, Le Verge R (1996) Controlled systemic absorption and increased anesthetic effect of bupivacaine following epidural administration of bupivacaine-hydroxypropyl-beta-cyclodextrin complex. Pharm Res 13:1576–1580

Garisto GA, Gaffen AS, Lawrence HP, Tenenbaum HC, Haas DA (2010) Occurrence of paresthesia after dental local anesthetic administration in the United States. J Am Dent Assoc 141:836–844

Giannakopoulos H, Levin LM, Secreto S, Moore PA, Peterson C, Hutcheson M, Bouhajib M, Mosenkis A, Townsend RR (2006) The pharmacokinetics and cardiovascular effects of high-dose articaine with 1:100.000 and 1:200.000 epinephrine. JADA 137:1562–1571

Giordano F, Novak C, Moyano JR (2001) Thermal analysis of cyclodextrins and their inclusion compounds. Thermochim Acta 380:123–151

Gouda R, Baishya H, Qing Z (2017) Application of mathematical models in drug release kinetics of carbidopa and levodopa ER tablets. J Dev Drugs 6:1–8

Haas DA (2006) Articaine and paresthesia: epidemiological studies. J Am Coll Dent 73:5–10

Haas DA, Lennon D (1995) A 21-year retrospective study of reports of paresthesias following local anesthetic administration. J Can Dent Assoc 61:319–330

Kambalimath DH, Dolas RS, Kambalimath HV, Agrawal SM (2013) Efficacy of 4% articaine and 2% lidocaine: a clinical study. J Maxillofac Oral Surg 12:3–10. https://doi.org/10.1007/s12663-012-0368-4

Kämmerer PW, Seeling J, Alshihri A, Daubländer M (2013) Comparative clinical evaluation of different epinephrine concentrations in 4% articaine for dental local infiltration anesthesia. Clin Oral Investig 6:1010–1017. https://doi.org/10.1007/s00784-013-1010-7

Kopecký F, Vojteková M, Kaclík P, Demko M, Bieliková Z (2004) Bupivacaine hydrochloride complexation with some alpha- and beta-cyclodextrins studied by potentiometry with membrane electrodes. J Pharm Pharmacol 56:581–587. https://doi.org/10.1211/0022357023295

Laverde A Jr, Conceiçao GJA, Queiroz SCN, Fujiwara FY, Marsaioli AJ (2002) An NMR tool for cyclodextrin selection in enantiomeric resolution by high-performance liquid chromatography. Magn Reson Chem 40:433–442. https://doi.org/10.1002/mrc.1043

Loftsson T, Duchêne D (2007) Cyclodextrins and their pharmaceutical applications. Int J Pharm 329:1–11

Loukas YL, Vraka V, Gregoriadis G (1998) Drugs in cyclodextrins in liposomes: a novel approach to the chemical stability of drugs sensitive to hydrolysis. Int J Pharm 162:137–142

Malamed SF, Gagnon S, Leblanc D (2001) Articaine hydrochloride: a study of the safety of a new amide local anesthetic. J Am Dent Assoc 132:177–185

Meier MM, Luiz MTB, Szpoganicz B, Soldi V (2001) Thermal analysis behavior of β and γ-cyclodextrin inclusion complexes with capric and caprilic acid. Thermochim Acta 375:153–160

Misiuk W, Zalewska M (2011) Spectroscopic investigations on the inclusion interaction between hydroxypropyl-β-cyclodextrin and bupropion. J Mol Liq 159:220–225

Moore PA, Haas DA (2010) Paresthesias in dentistry. Dent Clin N Am 54:715–730. https://doi.org/10.1016/j.cden.2010.06.016

Moraes CM, Abrami P, Araújo DR, Braga AFA, Issa MG, Ferraz HG, de Paula E, Fraceto LF (2007a) Characterization of lidocaine: hydroxypropyl-b-cyclodextrin inclusion complex. J Incl Phenom Macrocycl Chem 57:313–316

Moraes CM, Abrami P, de Paula E, Braga AFA, Fraceto LF (2007b) Study of the interaction between S(−) bupivacaine and 2-hydroxypropyl-beta-cyclodextrin. Int J Pharm 331:99–106. https://doi.org/10.1016/j.ijpharm.2006.09.054.b

Mosmann T (1983) Rapid colorimetric assay for cellular growth and survival: application to proliferation and cytotoxicity assays. J Immunol Methods 65:55–63

Mura P (2015) Analytical techniques for characterization of cyclodextrin complexes in the solid state: a review. J Pharm Biomed Anal 113:226–238. https://doi.org/10.1016/j.jpba.2015.01.058

Mura P, Maestrelli F, Cirri M, Furlanetto S, Pinzauti S (2003) Differential scanning calorimetry as an analytical tool in the study of drug-cyclodextrin interactions. J Therm Anal Calorim 73:635–646

Pellicer-Chover H, Cervera-Ballester J, Sanchis-Bielsa JM, Peñarrocha-Diago MA, Peñarrocha-Diago M, García-Mira B (2013) Comparative split-mouth study of the anesthetic efficacy of 4% articaine versus 0.5% bupivacaine in impacted mandibular third molar extraction. J Clin Exp Dent 5:66–71. https://doi.org/10.4317/jced.50869

Piccinni C, Gissi DB, Gabusi A, Montebugnoli L, Poluzzi E (2015) Paraesthesia after local anaesthetics: an analysis of reports to the FDA adverse event reporting system. Basic Clin Pharmacol Toxicol 117(1):52–56. https://doi.org/10.1111/bcpt.12357

Pinto LM, Fraceto LF, Santana MH, Pertinhez TA, Junior SO, de Paula E (2005) Physico-chemical characterization of benzocaine-beta-cyclodextrin inclusion complexes. J Pharm Biomed Anal 39:956–963. https://doi.org/10.1016/j.jpba.2005.06.010

Pogrel MA (2012) Permanent nerve damage from inferior alveolar nerve blocks: a current update. J Calif Dent Assoc 40:795–797

Prado AR, Yokaichiya F, Franco MKKD, Silva CMGD, Oliveira-Nascimento L, Franz-Montan M, Volpato MC, Cabeça LF, de Paula E (2017) Complexation of oxethazaine with 2-hydroxypropyl-β-cyclodextrin: increased drug solubility, decreased cytotoxicity and analgesia at inflamed tissues. J Pharm Pharmacol 69:652–662. https://doi.org/10.1111/jphp.12703

Ramteke KH, Dighe PA, Kharat AR, Patil SV (2014) Mathematical models of drug dissolution: a review. Sch Acad J Pharm 3(5):388–396

Serpe L, Franz-Montan M, Santos CP, Silva CB, Nolasco FP, Caldas CS, Volpato MC, Paula E, Groppo FC (2014) Anaesthetic efficacy of bupivacaine 2-hydroxypropyl-β-cyclodextrin for dental anaesthesia after inferior alveolar nerve block in rats. Br J Oral Maxillofac Surg 52:452–457. https://doi.org/10.1016/j.bjoms.2014.02.018

Shafi AAA, Shihry SS (2009) Fluorescence enhancement of 1-napthol-5-sulfonate by forming inclusion complex with β-cyclodextrin in aqueous solution. Spectrochim Acta 72:533–537. https://doi.org/10.1016/j.saa.2008.10.052

Shen J, Burgess DJ (2012) Accelerated in vitro release testing methods for extended release parenteral dosage forms. J Pharm Pharmacol 64:986–996. https://doi.org/10.1111/j.2042-7158.2012.01482.x

Sosnowska NS (1997) Fluorometric determination of association constants of three estrogens with cyclodextrins. J Fluoresc 7:195–200

Tortamano IP, Siviero M, Lee S, Sampaio RM, Simone JL, Rocha RG (2013) Onset and duration period of pulpal anesthesia of articaine and lidocaine in inferior alveolar nerve block. Braz Dent J 24:371–374. https://doi.org/10.1590/0103-6440201302072

Vermet G, Degoutin S, Chai F, Maton M, Bria M, Danel C, Hildebrand HF, Blanchemain N, Martel B (2014) Visceral mesh modified with cyclodextrin for the local sustained delivery of ropivacaine. Int J Pharm 476:149–159. https://doi.org/10.1016/j.ijpharm.2014.09.042

Xiliang G, Yu Y, Guoyan Z, Guomei Z, Jianbin C, Shaomin S (2003) Study on inclusion interaction of piroxicam with beta-cyclodextrin derivatives. Spectrochim Acta A Mol Biomol Spectrosc 59:3379–3386

Yilmaz VT, Karadag A, Icebudak H (1995) Thermal decomposition of β-cyclodextrin inclusion complexes of ferrocene and their derivatives. Thermochim Acta 261:107–118